Journal of Electronic Research and Application, 2022, Volume 6, Issue 2
http://ojs.bbwpublisher.com/index.php/JERA
ISSN Online: 2208-3510
ISSN Print: 2208-3502

Spectral Characteristic of Phosgene in External Electric Field

Huan An*, Mei Xiang*, Bumaliya Abulimiti*, Jingyan Zhen

School of Physics and Electronic Engineering, Xinjiang Normal University, Urumqi 830054, China

Corresponding authors: Huan An, huan950220@163.com; Mei Xiang, mei811014@126.com; Bumaliya Abulimiti, maryam917@163.com

---

Abstract: Phosgene is highly toxic, and it plays a role in the depletion of the ozone layer. The ground state geometric structure and spectral characteristic of phosgene in various external electric fields were calculated via the density-functional theory (DFT) and time-dependent density-functional theory (TDDFT) with the B3LYP/6-31+G(d) basis set. With external electric field, the structure of phosgene changed significantly. With increasing electric field, the bond lengths of 1C-3Cl and 1C-4Cl increased; the total energy and energy gap initially increased and then decreased, whereas the dipole moment initially decreased and then increased. Most of the IR vibrational frequencies were redshifted. The wavelength of the singlet excited state increased, reflecting a red shift, and the oscillator strengths of most transitions belonged to forbidden transitions. These results are of great significance for studying the dissociation of phosgene in external electric field.

Keywords: Density-functional theory; Phosgene; Spectrum characteristic; External electric field; Molecular dynamics

---

1. Introduction

The ozone layer absorbs harmful ultraviolet solar radiation, and thus protects human and the environment. In 1974, Molina's team of American scientists reported that Freon has a destructive effect on the ozone layer [1]. In 1985, Farman's team confirmed this at an Antarctic station, but there was still controversy concerning its mode of action [2]. In 2009, Zhimin Lin's team reported on the dissociation rate of ClOOCl, which provided clear evidence [3]. Two-body dissociation generally occurs in the lower atmosphere, while multi-body dissociation often occurs in the higher atmosphere, such as the stratosphere. In external electric field, molecules undergo a series of physical and chemical changes [4-6], such as molecular chemical bond breaking, molecular orbital, crystallization, and changes in excitation spectra [7-9]. In order to study the formation mechanism of chlorine free-radicals and to understand the effects of chlorinated compounds on the atmosphere, it is necessary to study the ground state geometry and spectral characteristic of chloride under external electric field.

Phosgene is widely used in the chemical industry as a reagent in the production of polyurethane, dyes, rubber, plastics, pesticides, and so on; it is closely related to human lives. In 2021, Patrick Vossnacker's team searched for new synthesis methods of phosgene [10]; however, it is found susceptible to hydrolysis, which generates chlorine free radicals that have a destructive chain reaction with the ozone layer ($Cl + O_3 \rightarrow ClO + O, ClO + O_3 \rightarrow Cl + 2O_2$) [11]. At present, the research on phosgene mainly includes phosgene toxicity [12,13], treatment methods after phosgene poisoning [14,15], and more on the detection methods of phosgene [16-18]. Scholars have neglected the harm caused by phosgene when in use; therefore, the problem of phosgene degradation needs to be solved urgently. At present, the only way to degrade phosgene is by thermal decomposition [19]. Degradation via external electric field is a new idea that has been applied to the study of halon molecules and methane derivatives [20-22]. The conditions required for electric field degradation are minimal, which is convenient for industrial applications. Due to the toxicity of phosgene, experimental research is inconvenient. Simultaneously, a theoretical study of phosgene in external electric field can reveal its ground-state geometric properties and spectral characteristic, which provide basic data for phosgene dissociation in external electric field. Therefore, it is of great significance to theoretically study the ground-state geometry properties and spectral characteristic of phosgene under the action of an external electric field. There have been few theoretical studies on the ground-state geometric properties and spectral characteristic of phosgene in external electric field.

Here, density-functional theory (DFT) and time-dependent density functional (TDDFT) with B3LYP/6-31+G(d) basis set were used to study the ground-state geometry properties and spectral characteristic of phosgene, providing a theoretical basis for its degradation via external electric fields (−0.05~0.05 a.u.). First, the ground-state geometry was optimized, including bond lengths, energy, dipole moment, energy-level distribution, and other physical parameters. Then, its infrared (IR) spectra were characterized. Those provided the basic parameters for the degradation of phosgene.

2. Theory and computational method

The Hamiltonian H of the phosgene molecular in applied electric field is given as follows:

$$H = H_0 + H_{\text{int}} \tag{1}$$

H_0 is the Hamiltonian without the electric field, and H_{int} is the Hamiltonian of the interaction between the electric field and the molecular system. Based on the dipole approximation, the interaction Hamiltonian between the molecular system and the electric field can be simplified as follows:

$$H_{\text{int}} = -\mu F \tag{2}$$

μ is the dipole moment of the molecule, and F is the electric field [6]. The convergence conditions were self-consistent-field and Davidson iterative. Self-consistent-field convergence involved a maximum force of ≤ 0.00045, a root-mean-square force of ≤ 0.0003, a maximum displacement of ≤ 0.0018, and a root-mean-square displacement of ≤ 0.001200. The Davidson iteration converged to the wave function variation of the n states, which was less than 0.001. All calculations were performed using the Gaussian 09 quantum computing software [23].

3. Results and discussion

3.1. Ground-state stable structure of phosgene

The calculated ground-state molecular structure model of phosgene was obtained at the lowest energy, as shown in **Figure 1**. Various methods and groups of phosgene molecules were optimized and calculated without an external electric field. The optimized vibrational frequencies were compared with the experimental values, as shown in **Table 1**. The vibrational frequencies obtained with the DFT B3LYP/6-31+G(d) basis set were consistent with the experimental data. Therefore, the DFT/B3LYP method and 6-31+G(d) basis set were also used for calculations of the molecule with an external electric field along the direction shown by the arrow in **Figure 1**.

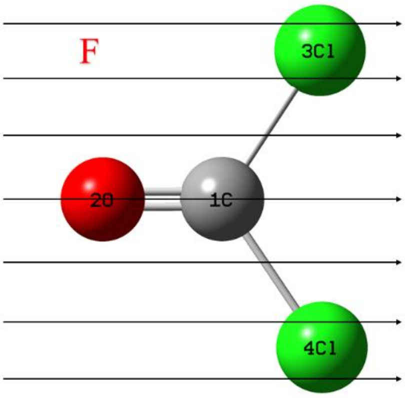

Figure 1. Stable structure of phosgene molecule

Table 1. Vibrational frequencies of phosgene molecule obtained using various methods

Vibration description	Calculated value/cm^{-1}					Experimental value/cm^{-1} [24]
	HF/6-31G	B3LYP/ 3-21G	B3LYP/ 6-31G	B3LYP/ 6-31+G(d)	B3LYP/ 6-311+G(d)	
CCl deform	303.96	264.99	279.58	303.44	302.09	285
CO deform	470.81	380.34	413.03	439.25	439.53	440
CCl s-str	560.16	468.77	505.73	561.56	555.54	567
C p-deform	605.04	530.79	542.64	583.43	585.56	580
CCl a-str	879.98	691.52	758.89	832.52	817.31	849
CO str	1961.88	1877.53	1819.36	1875.53	1879.37	1827

3.2. Geometric properties of phosgene in external electric field

The phosgene geometry structure was optimized for various external electric fields (−0.05~0.05 a.u.), which had significant effects.

3.2.1. Bond length

The effect on the bond length of phosgene in various electric fields is shown in **Figure 2**. The bond lengths of 1C-3Cl and 1C-4Cl increased with the electric field and were equivalent. In contrast, the 1C-2O bond length decreased with increasing electric field. The changes in the bond-length with electric field were attributed to the changes in the internal electric field [25]. With increasing external electric field, the charge transfer decreased the electric field, and the Coulomb forces became weaker between the 1C and the 3Cl atoms as well as the 1C and 4Cl atoms, decreasing the bond energies. Therefore, the 1C-3Cl and 1C-4Cl bond lengths increased, and their bond energies became weaker, easily breaking via the electric field. In contrast, with the external field, the 1C-2O bond was completely opposite, in which the 1C-2O bond length decreased and was less likely to break with increasing electric field.

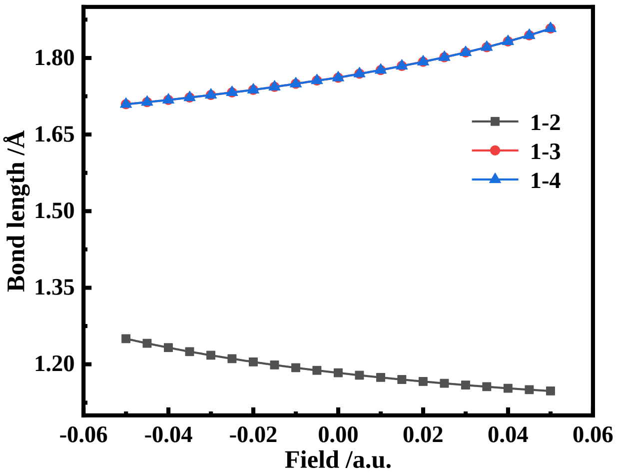

Figure 2. The bond length of phosgene molecule with external electric field

3.2.2. Total energy and dipole moment

The total energy and the dipole moment of phosgene were calculated with various external electric fields as shown in Figure 3. The total energy of the molecule initially increased and then decreased with the increase of electric field, while the dipole moment had changed oppositely. In view of the interaction between the intramolecular electric field and the external electric field, electrons in the molecule exhibited a directional shift. The negative charge moved along the opposite direction of the electric field, and the phosgene molecule was stretched. In other words, the molecule was polarized by the electric field, and the dipole moment decreased and then increased. On equation, $H_{int} = -\mu F$, the molecular dipole moment decreased initially and then increased, so the Hamiltonian increased initially and then decreased, and the total energy of the molecular increased initially and then decreased [22].

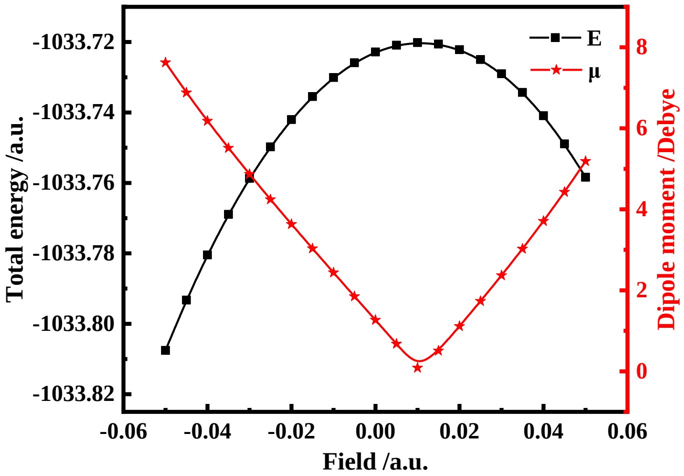

Figure 3. The total energy and the dipole moment of phosgene molecule with external electric field

3.2.3. Energy level distribution

Molecular frontier orbitals can determine many molecular properties, and thus they are important in physics and chemistry [26]. The lowest-unoccupied molecular orbital (LUMO) represents the molecular ability to obtain electrons, and lower values make it easier to obtain electrons. The highest-occupied molecular orbital (HOMO) is easily losing electrons, and higher values make it easier to lose electrons. This energy gap easily participates in chemical reactions, and smaller energy gaps make it easier to promote the molecule to the excited state and undergo chemical reactions.

The LUMO energy (E_L) and the HOMO energy (E_H) of the phosgene molecule were calculated for various external electric fields. The energy gap is given as follows:

$$E_G = (E_L - E_H) \times 27.2 eV \tag{3}$$

With increasing electric field, the molecular orbital of LUMO and HOMO changed significantly as shown in **Figure 4**. The LUMO and HOMO electrons were evenly distributed without electric field. With increasing electric field, the LUMO and HOMO electrons were transferred, especially those of LUMO. As the electrons were attracted to the external field, the HOMO electrons were almost distributed onto the 3Cl and 4Cl atoms. In **Figure 5**, E_L initially increased and then decreased, while E_H decreased slowly, which increased E_G initially and then decreased with the electric field. This shows that chemical reactions can occur when excited electrons easily leave an orbit and form a hole [27], which is consistent with the above conclusion.

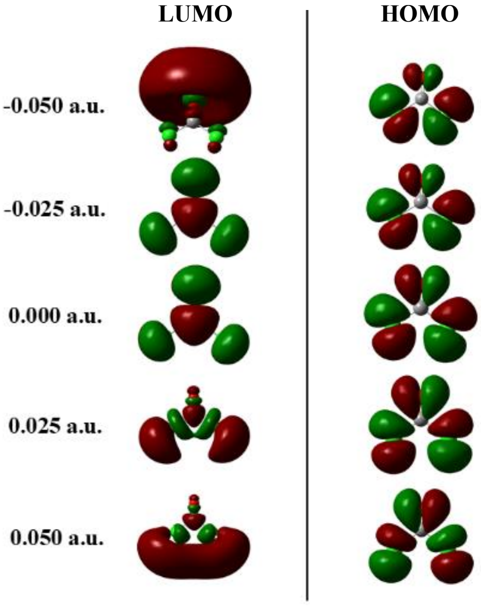

Figure 4. The frontier molecular orbital of phosgene molecule with external electric field

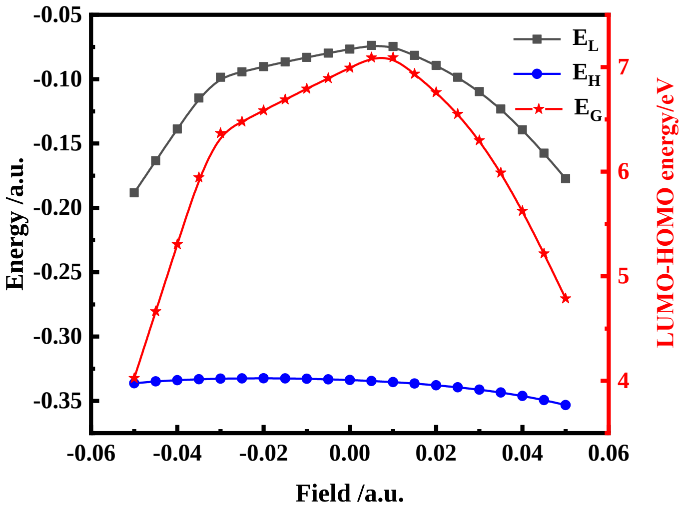

Figure 5. The energy level distribution of phosgene molecule with external electric field

3.3. Spectral characteristic of phosgene in external electric field

The spectral characteristic of a molecule is important for understanding its properties and structure. Various external electric fields (−0.05~0.05 a.u.) were applied along the direction of the arrow, and the phosgene molecular structure was optimized to calculate IR and Raman spectra. The spectral changed significantly in the electric field. The vibrational changes of the C-Cl bonds are of great significance when examining the dissociation mechanism of phosgene with external electric field. It is possible to speculate whether chemical bonds will break based on frequency changes.

Changes in the IR spectrum in the electric field are shown in **Figure 6**. The phosgene molecule has 6 vibrations. As shown in **Figure 6(a)**, the stretching vibration frequency of the 1C-2O bond (CO str) increased (blueshifted) with increasing electric field. With increasing electric field, the asynchronism stretching vibration frequency of the 1C-3Cl and 1C-4Cl bonds (CCl a-str) decreased (redshifted). The range over 250~600 cm^{-1} was expanded for a clearer visualization of the spectral shifts as shown in **Figure 6(b)**. As the electric field increased, the plane deformation vibration frequency of the C atom (C p-deform), the synchronism stretching vibration frequency of the 1C-3Cl and 1C-4Cl bonds (CCl s-str), the 1C-2O bond deformation vibration frequency (CO deform), and the deformation vibration frequency of the 1C-3Cl and 1C-4Cl bonds (CCl deform) all decreased; this means that they were redshifted.

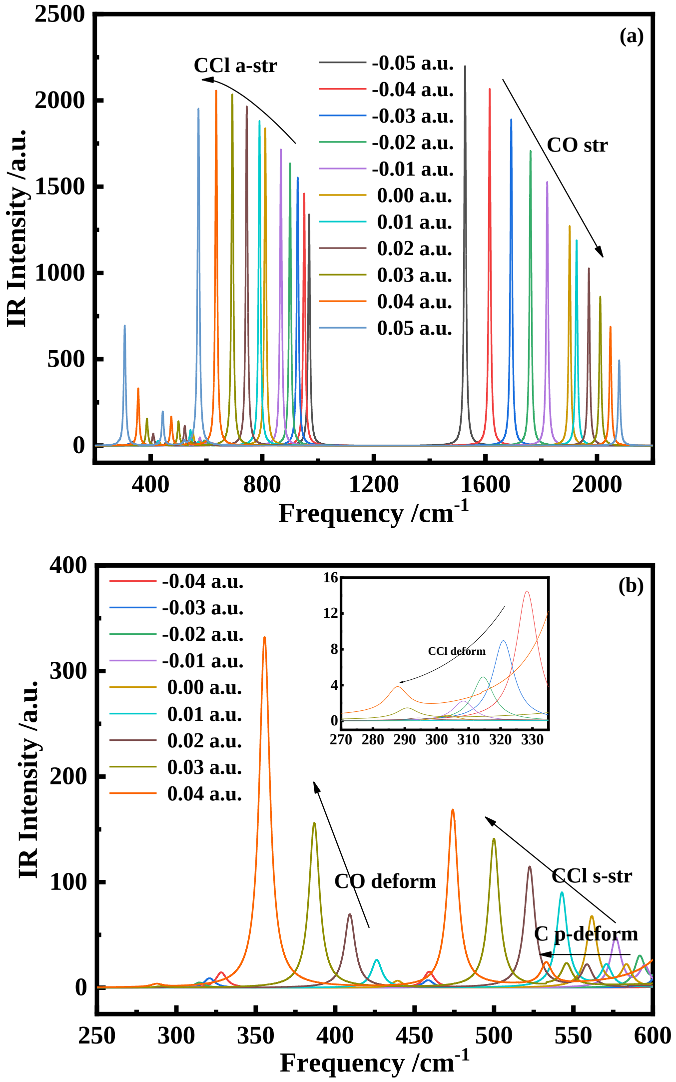

Figure 6. The IR spectrum of phosgene molecule with external electric field

3.4. Excited state of phosgene in external electric field

In order to further study the properties of phosgene, the transition selection rule $\Delta S = 0$, the wavelengths (λ), and oscillator strengths (*f*) of the first 10 singlet excited states of the molecule with external electric fields (0~0.05a.u.) were calculated using the TDDFT method B3LYP/6-31+G(D) basis set, as shown in **Table 2**. It can be seen from the data that the oscillator strengths of most transitions were equal to 0 or close to 0, thus belonging to forbidden transitions. The 1st and 5th excited states were in forbidden transitions under zero electric field and became allowed transitions when an external electric field was applied [28]. However, the second excited state was the opposite. With the increased of the external electric field, the wavelength basically increased (redshifted). Generally, the external electric field has a great influence on the properties of the excited states.

Table 2. Wavelength and oscillator intensity of singlet excited state of phosgene molecule with external electric field

State	**Field/a.u.**											
	0		**0.01**		**0.02**		**0.03**		**0.04**		**0.05**	
	λ/nm	***f***	**λ/nm**	***f***	**λ/nm**	***f***	**λ/nm**	***f***	**λ/nm**	***f***	**λ/nm**	***f***
n=1	232.30	0	227.14	0	236.36	0.0013	299.29	0.0071	469.34	0.0148	968.56	0.0297
n=2	202.38	0.0026	210.63	0.0080	231.31	0	277.14	0	423.26	0	867.27	0
n=3	200.39	0	194.73	0.0000	220.28	0	239.90	0.0001	290.30	0.1725	385.97	0.2074
n=4	186.87	0.0004	187.26	0.0288	206.14	0	226.03	0.1495	264.91	0.0017	314.89	0.0048
n=5	180.34	0	186.01	0	198.76	0.0360	224.18	0.0205	252.87	0.0004	296.34	0.0002
n=6	177.66	0	184.71	0	188.25	0.0408	211.95	0	250.33	0	290.57	0..0094
n=7	177.43	0	171.66	0.0091	184.91	0.1983	205.53	0	236.34	0.0121	282.40	0.0471
n=8	172.32	0.0513	171.16	0	180.96	0.0033	203.49	0.0503	232.59	0.0332	265.14	0.0016
n=9	164.68	0.0083	167.82	0.0297	175.49	0.0422	199.37	0.0112	217.65	0.0003	259.74	0.0065
n=10	161.82	0.4332	165.51	0.3574	175.40	0.0002	195.30	0.0573	213.64	0.0706	245.26	0

4. Conclusion

The ground-state geometric structure, the spectral characteristic, and singlet excited state of phosgene in various external electric fields (−0.05~0.05 a.u.) were calculated via DFT or TDDFT with the B3LYP/6–31+G(d) basis set. The effect of electric field on the bond length, total energy, dipole moment, energy-level orbital distribution, LUMO-HOMO energy gap, IR spectra, as well as the wavelength and oscillator intensity of the singlet excited state was analyzed. The phosgene structure changed significantly in the electric field. With increasing electric field, the 1C-2O bond length decreased, while the 1C-3Cl and 1C-4Cl bond lengths increased. In the electric field, the total energy of the molecule first increased and then decreased, while the dipole moment changes were opposite; the LUMO-HOMO gap first increased and then decreased. With increasing electric field, most of the IR vibrational frequencies were redshifted. The wavelength of the singlet excited state increased, reflecting a redshift. The oscillator strengths of most transitions were equal to 0 or close to 0, thus belonging to forbidden transitions. The calculated ground-state geometric data, spectral characteristic, and the singlet excited state of phosgene indicate that it can be decomposed by external electric field. This will provide theoretical guidance for investigations of the dissociation of phosgene.

Funding

(1) National Natural Science Foundation of China (Grant Number: 21763027);

(2) Innovation Team for Monitoring of Emerging Contaminants and Biomarkers (Grant Number: 2021D14017);

(3) Xinjiang Regional Collaborative Innovation Project (Grant Number: 2019E0223);

(4) Scientific Research Program of Colleges and Universities in Xinjiang (Grant Number: XJEDU2020Y029);

(5) "13th Five-Year" Plan for Key Discipline Physics Bidding Project of Xinjiang Normal University (Grant Number: 17SDKD0602).

Disclosure statement

The authors declare no conflict of interest.

References

[1] Molina MJ, Rowland FS, 1974, Stratospheric Sink for Chlorofluoromethanes: Chlorine Atomc-Atalysed Destruction of Ozone. Nature, 249(5460): 810-812.

[2] Zhang ZM, 1999, Who Discovered the Ozone Hole?. Friends of Chemical Industry, 39(02): 45.

[3] Chen HY, Lien CY, Lin WY, 2009, UV absorption Cross Sections of Cloocl Are Consistent with Ozone Degradation Models. Science, 324(5928): 781.

[4] Lan YC, Wang H, Wu LX, et al., 2012, Electroreduction of Dibromobenzenes on Silver Electrode in the Presence of CO_2. Journal of Electroanalytical Chemistry, 664(15): 33-38.

[5] Wu HY, 2006, Analysis of Halon Substitute Agent Environment Affection and Study on Extinguishing System of Halon Substitutes, Tianjin University, Tianjin.

[6] Li XH, Liu YZ, Chen YY, et al., 2018, Investigation on Molecular Properties of Freon 13 in External Electric Field. Journal of Molecular Science, 34(2): 139-143.

[7] Xu HP, Ying YH, 2016, The molecular Structure and Properties of Agcl Under External Electric Field. Journal of Atomic and Molecular Physics, 33(1): 1-7.

[8] Zhou ZY, Liu YZ, Li J, et al., 2017, Influence of External Electric Field on the Molecular Structure and Electronic Spectrum of Formaldehyde Molecule. Journal of Molecular Science, 33(3): 217-224.

[9] Wang JP, Zhai DD, Ma P, et al., 2020, Theoretical Insight into the Effects of External Electric Field on Cocrystal HMX/DMI. Journal of Propellants and Explosives, 43(2): 133-138.

[10] Vossnacke P, Wust A, Keilhack T, et al., 2021, Novel Synthetic Pathway for the Production of Phosgene. Science Advances, 7(40): 5186.

[11] Li J, Liu YZ, Yin WY, et al., 2017, Spectra and Dissociation Properties of Freon 31 Under Electric Field. Spectroscopy Letters, 50(10): 572-578.

[12] Hobson ST, Casillas RP, Richieri RA, et al., 2019, Development of an Acute, Short-Term Exposure Model for Phosgene. Toxicology Mechanisms and Methods, 29(8): 604-615.

[13] Olivera DS, Hoard-Fruchey H, Sciuto AM, 2016, Evaluation of an in Vitro Screening Model to Assess Phosgene Inhalation Injury. Toxicology Methods, 27(1): 45-51.

[14] Hobson ST, Richieri RA, Parseghian MH, 2021, Phosgene: Toxicology, Animal Models, and Medical Countermeasures. Toxicology Mechanisms and Methods, 31(4): 293-307.

[15] Lu QY, Huang SY, Meng XY, et al., 2021, Mechanism of Phosgene-Induced Acute Lung Injury and Treatment Strategy. International Journal of Molecular Sciences, 22(20): 10933.

[16] Pitschmann V, Matejovsky L, Zeman J, et al., 2020, Second-Generation Phosgene and Diphosgene Detection Tube. Chemosensors, 8(4): 107.

[17] Khan S, Sajid H, Ayub K, et al., 2020, High Sensitivity of Graphdiyne Nanoflake toward Detection of Phosgene, Thiophosgene and Phosogenoxime; A First-Principles Study. Journal of Molecular Graphics and Modelling, 100(prepublish): 107658.

[18] Wang SL, Zhong L, Song QH, 2018, Sensitive and Selective Detection of Phosgene, Diphosgene, and Triphosgene by a 3,4-Diaminonaphthalimide in Solutions and the Gas Phase. Chemistry (Weinheim an der Bergstrasse, Germany), 24(21): 5652-5658.

[19] Carlos LHJ, Baptiste S, Laurent V, et al., 2018, Thermal Decomposition of Phosgene and Diphosgene. The Journal of Physical Chemistry A, 122(1): 249-257.

[20] Liu YZ, Li XH, Wang JF, et al., 2017, Study on Dissociation Properties and Spectra of Halon 1301 in External Electric Field. Spectroscopy and Spectral Analysis, 37(03): 679-684.

[21] Zhang XYZ, Liu YZ, Ma XY, 2018, Dissociation and Physical Properties of Methyl Iodide in External Electric Field. Journal of University of Chinese Academy of Sciences, 35(06): 839-844.

[22] Wu YG, Liu JX, Liu HL, et al., 2019, Spectrum and Dissociation Properties of Fluoro Trichloro Methane Molecule in Radiational Field. Acta Physical Sonica, 68(06): 64-72.

[23] Frish MJ, Trucks GW, Schlegel HB, et al., 2010, Gaussian 09, Revision C. 01., Gaussian, Inc., Wallingford.

[24] Shimanouchi T, 1977, Tables of Molecular Vibrational Frequencies. Consolidated. Volume II. Journal of Physical and Chemical Reference Data, 6(3): 103.

[25] Zhu ZH, 1991, Atomic and Molecular Reaction Statics, Science Press, Beijing.

[26] Cardona CM, Li W, Kaifer AE, et al., 2011, Electrochemical Considerations for determining Absolute Frontier Orbital Energy Levels of Conjugated Polymers for Solar Cell Applications. Advanced Materials, 23(20): 2367-2371.

[27] Li J, Liu YZ, Cheng QY, et al., 2017, Study on the Physical Characteristics of Halon-1211 Under the Electrical Fields. Journal of Atomic and Molecular Physics, 34(6): 1017-1024.

[28] Yin YH, Wang L, 2017, Structure and Properties of AgBr Molecule Under External Electric Field. Journal of Atomic and Molecular Physics, 34(1): 9-15.